

# Spatial distribution of Cherenkov radiation in periodic dielectric media

**Christian Kremers and Dmitry N. Chigrin**

Theoretical Nano-Photonics, Institute of High-Frequency and Communication Technology, Faculty of Electrical, Information and Media Engineering, University of Wuppertal, Rainer-Gruenter-Str. 21, D-42119 Wuppertal, Germany

E-mail: [kremers@uni-wuppertal.de](mailto:kremers@uni-wuppertal.de)

**Abstract.** The nontrivial dispersion relation of a periodic medium affects both the spectral and the spatial distribution of Cherenkov radiation. We present a theory of the spatial distribution of Cherenkov radiation in the far-field zone inside arbitrary three- and two-dimensional dielectric media. Simple analytical expressions for the far-field are obtained in terms of the Bloch mode expansion. Numerical examples of the Cherenkov radiation in a two-dimensional photonic crystal is presented. The developed analytical theory demonstrates good agreement with numerically rigorous finite-difference time-domain calculations.

## 1. Introduction

In recent years light-matter interaction in inhomogeneous media, structured on the sub-wavelength scale, has attracted a considerable attention. The interplay between interference and propagation can result in a nontrivial dispersion relation in such a medium. For example, in a periodic dielectric medium [1, 2] both dispersion and diffraction of electromagnetic waves are substantially modified leading to novel optical phenomena, including the emission dynamics modification [3, 4, 5], ultra-refraction [6, 7, 8, 9] and photon focusing [10, 11, 12] effects. A nontrivial dispersion relation can also substantially modify the Cherenkov radiation [13, 14, 15]. For example an electron moving in a homogeneous medium with dispersion can emit at any velocity [15] and the spatial distribution of the emitted radiation demonstrates intensity oscillations behind the Cherenkov cone [16, 17, 18].

Periodic media modify both spectral [26, 27] and spatial [26] distribution of the Cherenkov radiation. At the moment, several studies on the modification of the Cherenkov and Smith-Purcell radiation are available. The Smith-Purcell radiation has been studied in Refs. [19, 20, 21, 22, 23]. The Cherenkov radiation has been used to map a band structure of a two-dimensional (2D) photonic crystal in Refs. [24, 25]. We have recently presented a general theory of spectral power modification in both three-dimensional (3D) and 2D periodic media [27]. Spatial modifications of the Cherenkov radiation have been numerically analyzed in Ref. [26] using the finite-difference time-domain (FDTD) method.

The main purpose of the present work is to develop an analytical theory of the Cherenkov radiation in far-field zone in order to provide a simple semi-analytical tool to study its spatial distribution peculiarities in general 3D and 2D periodic dielectric media. To achieve this goal we first derive an analytical expression for the electric far-field in terms of the Bloch mode expansion. Secondly we restrict the full  $k$ -space integration in the Bloch mode expansion of the field to a relatively simple surface (contour) integral in the first Brillouin zone of the 3D (2D) periodic medium. Thirdly, we restrict this integral further to a simple sum over a small number of Bloch eigenmodes. These derived formulas allow us to identify the main contribution to the spatial peculiarities of the Cherenkov radiation.

The paper is organized as follows: In Section 2 the general solution of Maxwell's equations is summarized. In Section 3 an analytical expression for the Cherenkov far-field is derived both for 3D and 2D periodic dielectric media. In Section 4 we apply the developed theory to calculate the Cherenkov far-field in the particular case of a 2D photonic crystal. Predictions of the analytical theory are substantiated by numerically rigorous FDTD calculations. Section 5 concludes the paper.

## 2. General solution

We consider a point (line) charge  $q$  uniformly moving with a velocity  $\mathbf{v}$  in an infinite periodic 3D (2D) dielectric medium (Fig. 1). The medium is described by a periodic dielectric function  $\varepsilon(\mathbf{r}) = \varepsilon(\mathbf{r} + \mathbf{R})$  with  $\mathbf{R} = \sum_i l_i \mathbf{a}_i$  being a vector of the direct Bravais lattice. The  $l_i$  are integers and the  $\mathbf{a}_i$  are basis vectors of the lattice. We assume also that the medium is linear, nonmagnetic and loss less. The relevant part of Maxwell's equations read in SI units:

$$\nabla \times \mathbf{E}(\mathbf{r}, t) = -\mu_0 \frac{\partial}{\partial t} \mathbf{H}(\mathbf{r}, t), \quad (1)$$

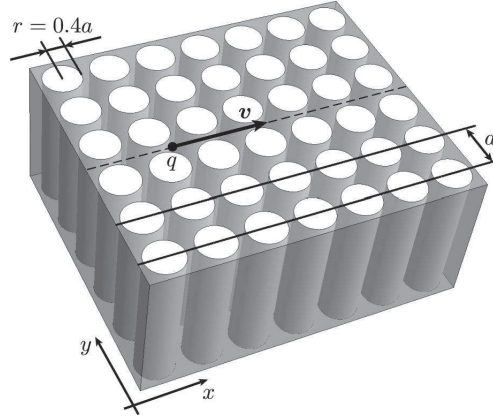


**Figure 1.** A sketch of a periodic medium and charge trajectory. Parameters of the infinite 2D photonic crystal used in the numerical example (Sec. 4) are shown.

$$\nabla \times \mathbf{H}(\mathbf{r}, t) = \varepsilon_0 \varepsilon(\mathbf{r}) \frac{\partial}{\partial t} \mathbf{E}(\mathbf{r}, t) + \mathbf{J}(\mathbf{r}, t), \quad (2)$$

where  $\mathbf{E}(\mathbf{r}, t)$  is the electric field,  $\mathbf{H}(\mathbf{r}, t)$  is the magnetic field and  $\mathbf{J}(\mathbf{r}, t)$  is the current density. In the presence of an arbitrary current density switched on adiabatically  $\mathbf{J}(\mathbf{r}, t \rightarrow -\infty) = 0$ , a general solution of Maxwell's equations (1-2) for the electric field at point  $\mathbf{r}$  and time  $t$  can be given in terms of the Bloch eigenmode expansion [2, 28]

$$\mathbf{E}(\mathbf{r}, t) = -\frac{1}{(2\pi)^d \varepsilon_0} \sum_n \int_{\text{BZ}} d^d k \int d^d r' \int_{-\infty}^t dt' \left\{ \cos \left[ \omega_{\mathbf{k}n}^{(T)}(t - t') \right] \cdot \mathbf{E}_{\mathbf{k}n}^{(T)}(\mathbf{r}) \otimes \mathbf{E}_{\mathbf{k}n}^{(T)*}(\mathbf{r}') + \mathbf{E}_{\mathbf{k}n}^{(L)}(\mathbf{r}) \otimes \mathbf{E}_{\mathbf{k}n}^{(L)*}(\mathbf{r}') \right\} \cdot \mathbf{J}(\mathbf{r}', t'). \quad (3)$$

$d = 2, 3$  is the dimensionality of the periodic lattice. The asterisk ( $\star$ ) and  $\otimes$  denote the complex conjugate and the outer tensor product, respectively.  $\mathbf{E}_{\mathbf{k}n}^{(T)}(\mathbf{r})$  and  $\mathbf{E}_{\mathbf{k}n}^{(L)}(\mathbf{r})$  are generalized transverse and longitudinal Bloch eigenmodes [2, 28] characterized by the band index  $n$ , the wave vector  $\mathbf{k}$  and the eigenfrequencies  $\omega_{\mathbf{k}n}^{(T)}$  and  $\omega_{\mathbf{k}n}^{(L)}$ , where  $\omega_{\mathbf{k}n}^{(L)} = 0$ . The  $k$ -space integration is performed over the first Brillouin zone (BZ) of the periodic lattice and the summation is carried out over the different photonic bands. Bloch eigenmodes are solutions of the homogeneous wave equation and satisfy periodic boundary conditions. These eigenmodes are normalized

$$\int d^d r \varepsilon(\mathbf{r}) \mathbf{E}_{\mathbf{k}n}^{(\alpha)*}(\mathbf{r}) \cdot \mathbf{E}_{\mathbf{k}'n'}^{(\beta)}(\mathbf{r}) = (2\pi)^d \delta_{\alpha\beta} \delta_{nn'} \delta^{(d)}(\mathbf{k} - \mathbf{k}') \quad (4)$$

and satisfy the completeness relation

$$\begin{aligned} & \sum_{n\alpha} \int_{\text{BZ}} d^d k \sqrt{\varepsilon(\mathbf{r}) \varepsilon(\mathbf{r}')} \mathbf{E}_{\mathbf{k}n}^{(\alpha)}(\mathbf{r}) \otimes \mathbf{E}_{\mathbf{k}n}^{(\alpha)*}(\mathbf{r}') \\ & = (2\pi)^d \mathbb{1} \delta^{(d)}(\mathbf{r} - \mathbf{r}'), \end{aligned} \quad (5)$$

where  $\alpha, \beta = T$  or  $L$ , and  $\mathbb{1}$  is the unit tensor.

For a point (line) charge  $q$  moving with the velocity  $\mathbf{v}$ , the current density  $\mathbf{J}(\mathbf{r}, t)$  can be expressed as

$$\mathbf{J}(\mathbf{r}, t) = q\mathbf{v} \delta^{(d)}(\mathbf{r} - \mathbf{v}t). \quad (6)$$

Using this current density and performing the space integration in the Bloch eigenmode expansion (3) the following general solution can be obtained

$$\mathbf{E}(\mathbf{r}, t) = -\frac{q|\mathbf{v}|}{(2\pi)^d \varepsilon_0} \sum_n \int_{\text{BZ}} d^d k \int_{-\infty}^t dt' \cos[\omega_{\mathbf{k}n}^{(T)}(t-t')] \cdot \mathbf{E}_{\mathbf{k}n}^{(T)}(\mathbf{r}) \left( \mathbf{E}_{\mathbf{k}n}^{(T)*}(\mathbf{v}t') \cdot \hat{\mathbf{v}} \right) \quad (7)$$

with  $\hat{\mathbf{v}} = \mathbf{v}/|\mathbf{v}|$  being the unit vector in the direction of the charge velocity. Here the fact that the longitudinal modes do not contribute to the radiated field [27] has been taken into account. In what follows the upper index ( $T$ ) denoting transverse eigenmodes and eigenfrequencies will be dropped.

### 3. Cherenkov radiation in the far-field zone

Expressing the cosine function in Eq. (7) as a sum of two complex exponential functions and using Bloch's theorem  $\mathbf{E}_{\mathbf{k}n}(\mathbf{r}) = \mathbf{e}_{\mathbf{k}n}(\mathbf{r}) \exp(i\mathbf{k} \cdot \mathbf{r})$ , where  $\mathbf{e}_{\mathbf{k}n}(\mathbf{r})$  is a lattice periodic function [2], a general solution for the Cherenkov field can be rewritten in the form

$$\mathbf{E}(\mathbf{r}, t) = -\frac{q|\mathbf{v}|}{2(2\pi)^d \varepsilon_0} \sum_n (I_+ + I_-) \quad (8)$$

where  $I_{\pm}$  is defined as

$$I_{\pm} = \int_{\text{BZ}} d^d k \int_{-\infty}^t dt' \mathbf{e}_{\mathbf{k}n}(\mathbf{r}) (\mathbf{e}_{\mathbf{k}n}^*(\mathbf{v}t') \cdot \hat{\mathbf{v}}) \mathcal{E}_{\pm}(\mathbf{k}, t') \quad (9)$$

with

$$\mathcal{E}_{\pm}(\mathbf{k}, t') = \exp\{i[\mathbf{k} \cdot (\mathbf{r} - \mathbf{v}t') \pm \omega_{\mathbf{k}n}(t-t')]\}. \quad (10)$$

Further taking into account the symmetries of the Bloch eigenmodes,  $\mathbf{e}_{-\mathbf{k}n} = \mathbf{e}_{\mathbf{k}n}^*$  and  $\omega_{-\mathbf{k}n} = \omega_{\mathbf{k}n}$  [2], the following relation for the integrals  $I_{\pm}$  (9) holds

$$\begin{aligned} I_-^* &= \int_{\text{BZ}} d^d k \int_{-\infty}^t dt' \mathbf{e}_{-\mathbf{k}n}(\mathbf{r}) (\mathbf{e}_{-\mathbf{k}n}^*(\mathbf{v}t') \cdot \hat{\mathbf{v}}) \mathcal{E}_+(-\mathbf{k}, t') \\ &= I_+. \end{aligned} \quad (11)$$

Therefore the radiated field (8) can be exclusively expressed in terms of the real part of the integral  $I_-$

$$\mathbf{E}(\mathbf{r}, t) = -\frac{q|\mathbf{v}|}{(2\pi)^d \varepsilon_0} \sum_n \text{Re}(I_-). \quad (12)$$

To analyze further the Cherenkov field (12) we limit ourselves to the charge trajectories which do not cut dielectric interfaces of the periodic medium. In this case ‘‘bremsstrahlung’’ radiation can be neglected and the trajectories themselves are necessarily oriented rationally with respect to the periodic lattice. In this case  $\mathbf{e}_{\mathbf{k}n}^*(\mathbf{v}t') \cdot \hat{\mathbf{v}}$  in (9) is a one-dimensional (1D) periodic function with a period  $\mathbf{a}$  defined by the orientation of the charge trajectory therefore one can Fourier expand it as follows

$$\mathbf{e}_{\mathbf{k}n}^*(\mathbf{v}t') \cdot \hat{\mathbf{v}} = \sum_{m=-\infty}^{\infty} c_{nm}(\mathbf{k}) \exp\left(i \frac{2\pi|\mathbf{v}|}{\mathbf{a}} m t'\right) \quad (13)$$

with Fourier coefficients

$$c_{nm}(\mathbf{k}) = \frac{1}{\mathbf{a}} \int_0^{\mathbf{a}} d\xi (\mathbf{e}_{\mathbf{k}n}^*(\xi \hat{\mathbf{v}}) \cdot \hat{\mathbf{v}}) \exp\left(-i \frac{2\pi}{\mathbf{a}} m \xi\right). \quad (14)$$

This allows us to rewrite (9) in the form

$$I_- = \sum_{m=-\infty}^{\infty} \int_{\text{BZ}} d^d k \int_{-\infty}^t dt' \mathbf{e}_{\mathbf{k}n}(\mathbf{r}) c_{nm}(\mathbf{k}) \tilde{\mathcal{E}}_{nm}(\mathbf{k}, t') \quad (15)$$

with function  $\tilde{\mathcal{E}}_{nm}(\mathbf{k}, t')$  defined by

$$\begin{aligned} \tilde{\mathcal{E}}_{nm}(\mathbf{k}, t') &= \exp\left[i\left(\mathbf{k} \cdot (\mathbf{r} - \mathbf{v}t') - \omega_{\mathbf{k}n}(t - t') + \frac{2\pi|\mathbf{v}|}{\mathbf{a}} m t'\right)\right] \\ &= \exp[i f_{nm}(\mathbf{k}, t')]. \end{aligned} \quad (16)$$

We are interested in the field far away from the trajectory of the charge. In the far-field zone the following relation  $|\mathbf{r} - \mathbf{v}t'| \gg \lambda$  holds for all moments of time  $t' \leq t$ . If this condition is fulfilled a small variation of wave vector  $\mathbf{k}$  results in rapid oscillations of the exponential function  $\tilde{\mathcal{E}}_{nm}(\mathbf{k}, t')$ . Taking into account that the function  $\mathbf{e}_{\mathbf{k}n}(\mathbf{r}) c_{nm}(\mathbf{k})$  is a slow function of the wave vector, the main contribution to the integral  $I_-$  in the far-field zone comes from the neighborhood of  $k$ -points where the variation of the phase  $f_{nm}(\mathbf{k}, t')$  is minimal. Such stationary  $k$ -points are defined by the relation

$$\nabla_{\mathbf{k}} f_{nm}(\mathbf{k}, t') = 0, \quad (17)$$

which explicitly reads as

$$\mathbf{v}_g(\mathbf{k}) = \nabla_{\mathbf{k}} \omega_n(\mathbf{k}) = \frac{\mathbf{r} - \mathbf{v}t'}{t - t'}. \quad (18)$$

Where  $\mathbf{v}_g(\mathbf{k})$  is the group velocity of the Bloch eigenmode. Relation (18) can be written in the equivalent form

$$(\mathbf{v}_g(\mathbf{k}) - \mathbf{v}) \cdot (\mathbf{r} - \mathbf{v}t) = \frac{|\mathbf{r} - \mathbf{v}t'|^2}{t - t'}, \quad (19)$$

with its right hand side being positive for all moments of time  $t' < t$ . Taking that into account, the integration in (15) can be restricted to the part of the Brillouin zone,  $\text{BZ}_1$ , containing all wave vectors whose group velocities fulfill the relation

$$(\mathbf{v}_g(\mathbf{k}) - \mathbf{v}) \cdot (\mathbf{r} - \mathbf{v}t) > 0. \quad (20)$$

Further, noting that in  $\text{BZ}_1$  there does not exist any stationary points for  $t' > t$ , the  $t'$ -integration in (15) can be extended to the whole real axis without severe error. With a good accuracy the integral  $I_-$  can be approximated by

$$I_- \approx \sum_{m=-\infty}^{\infty} \int_{\text{BZ}_1} d^d k \int_{-\infty}^{\infty} dt' \mathbf{e}_{\mathbf{k}n}(\mathbf{r}) c_{nm}(\mathbf{k}) \tilde{\mathcal{E}}_{nm}(\mathbf{k}, t'). \quad (21)$$

Using the integral expression of the Dirac delta function, the  $t'$ -integration can be easily performed resulting in

$$\begin{aligned} I_- &\approx 2\pi \sum_{m=-\infty}^{\infty} \int_{\text{BZ}_1} d^d k \mathbf{e}_{\mathbf{k}n}(\mathbf{r}) c_{nm}(\mathbf{k}) \exp[i(\mathbf{k} \cdot \mathbf{r} - \omega_{\mathbf{k}n} t)] \\ &\quad \cdot \delta\left(\omega_{\mathbf{k}n} - \mathbf{k} \cdot \mathbf{v} + \frac{2\pi|\mathbf{v}|}{\mathbf{a}} m\right). \end{aligned} \quad (22)$$

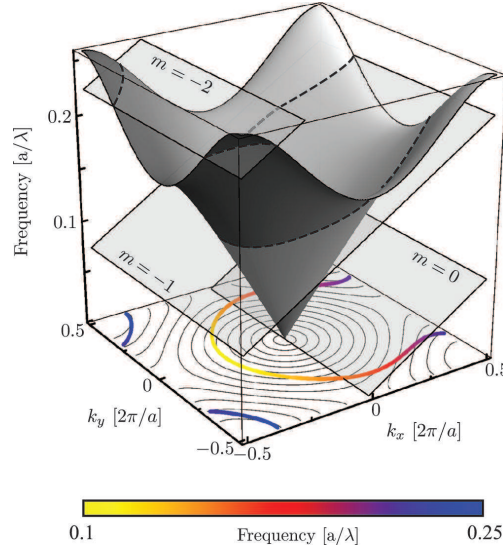


**Figure 2.** Diagram to illustrate the generalized Cherenkov condition. The band structure of the 2D photonic crystal (Fig. 2) for TE (transverse electric) polarization as well as the set of planes for  $m = 0$ ,  $m = -1$  and  $m = -2$  and the charge velocity  $\mathbf{v} = 0.15c \hat{\mathbf{x}}$  are shown. The intersections of the band structure with the planes define the integration contour  $\mathcal{C}_m$  (dashed lines). A color coded projection of the contour on the first Brillouin zone is also shown.

Furthermore, using the integral relation

$$\int_V d^d r f(\mathbf{r}) \delta(g(\mathbf{r})) = \int_{\partial V} d^{d-1} r \frac{f(\mathbf{r})}{|\nabla g(\mathbf{r})|},$$

where  $\partial V$  is a surface defined by the equation  $g(\mathbf{r}) = 0$ , the  $d$ -dimensional integral in (22) can be reduced to the  $(d-1)$ -dimensional integral

$$I_- \approx 2\pi \sum_m \int_{\mathcal{C}_m} d^{d-1} k \frac{e_{\mathbf{k}n}(\mathbf{r}) c_{nm}(\mathbf{k})}{|\mathbf{v}_g(\mathbf{k}) - \mathbf{v}|} \exp[i(\mathbf{k} \cdot \mathbf{r} - \omega_{\mathbf{k}n} t)], \quad (23)$$

which finally gives the following expression for the Cherenkov far-field

$$\mathbf{E}(\mathbf{r}, t) = - \frac{q |\mathbf{v}|}{(2\pi)^{d-1} \varepsilon_0} \sum_{n,m} \text{Re} \left\{ \int_{\mathcal{C}_m} d^{d-1} k \frac{e_{\mathbf{k}n}(\mathbf{r}) c_{nm}(\mathbf{k})}{|\mathbf{v}_g(\mathbf{k}) - \mathbf{v}|} \cdot \exp[i(\mathbf{k} \cdot \mathbf{r} - \omega_{\mathbf{k}n} t)] \right\}. \quad (24)$$

The integration is performed over the part of the Brillouin zone,  $\text{BZ}_1$ , defined by (20) and the integration surface (3D case) or contour (2D case)  $\mathcal{C}_m$  is defined by the generalized Cherenkov condition [27]

$$\omega_{\mathbf{k}n} = \mathbf{k} \cdot \mathbf{v} - \frac{2\pi}{a} m |\mathbf{v}|, \quad (25)$$

where  $m$  is an integer. In what follows we will refer to the integration surface (contour) (25) as Cherenkov surface (contour).

Equation (24) is the main result of the present section. We have demonstrated that a restriction of the integration range from the whole Brillouin zone to the solutions

of the generalized Cherenkov condition (25) in BZ<sub>1</sub> (20) is possible. The generalized Cherenkov condition (25) chooses all Bloch modes contributing to the Cherenkov radiation. A graphical illustration of the Cherenkov condition (25) is presented in figure 2. The band structure of an infinite square lattice photonic crystal is shown. The dielectric constant of the background medium is  $\varepsilon = 12$  and the radius of the air holes is  $r = 0.4a$ , where  $a$  is the lattice constant (Fig. 1). The manifold of the Cherenkov wave vectors (the integration contour  $\mathcal{C}_m$ ) is given by the intersection of the band structure,  $\omega_{\mathbf{k}n}$ , with the set of planes  $f(\mathbf{k}_{\parallel}) = |\mathbf{v}| \mathbf{k}_{\parallel} - |\mathbf{v}| \frac{2\pi}{a} m$  for different  $m$ . Here  $\mathbf{k}_{\parallel}$  is the component of the wave vector parallel to the charge velocity. The slope of the planes is defined by the charge velocity, being  $\mathbf{v} = 0.15c \hat{\mathbf{x}}$  in this example.

### 3.1. 2D periodic media

To further simplify the integral (23) we can parameterize the contour  $\mathcal{C}_m$  by its arc length  $s$ . Then the contour integral (23) with  $d = 2$  can be transformed into an integral over  $s$

$$I_- \approx 2\pi \sum_m \int ds \frac{e_n(\mathbf{k}(s), \mathbf{r}) c_{nm}(\mathbf{k}(s))}{|\mathbf{v}_g(\mathbf{k}(s)) - \mathbf{v}|} \cdot \exp\{i[\mathbf{k}(s) \cdot \mathbf{r} - \omega_n(\mathbf{k}(s))t]\}. \quad (26)$$

The main contribution to the integral comes from the  $k$ -points  $\mathbf{k}(s^\nu)$  in whose neighborhood the phase  $h(s) = \mathbf{k}(s) \cdot \mathbf{r} - \omega_n(\mathbf{k}(s))t$  is stationary with respect to the variation of  $s$

$$\begin{aligned} \left. \frac{\partial}{\partial s} [\mathbf{k}(s) \cdot \mathbf{r} - \omega_n(\mathbf{k}(s))t] \right|_{s=s^\nu} &= 0 \\ (\mathbf{r} - \mathbf{v}t) \cdot \frac{\partial \mathbf{k}^\nu}{\partial s} &= 0. \end{aligned} \quad (27)$$

The second equality in (27) holds as the derivative of the Cherenkov condition (25) with respect to the arc length  $s$  results in

$$(\mathbf{v}_g(\mathbf{k}(s)) - \mathbf{v}) \cdot \frac{\partial \mathbf{k}}{\partial s} = 0. \quad (28)$$

Combining the stationary phase condition (27) with relation (28) and taking into account the definition of BZ<sub>1</sub> (20), one can see that for the stationary Bloch modes the vector  $\mathbf{v}_g(\mathbf{k}^\nu) - \mathbf{v}$  must be parallel to the vector  $\mathbf{r} - \mathbf{v}t$ . In other words, only the eigenmodes whose group velocities in the coordinate frame moving with the point (line) charge pointing towards an observation direction in this coordinate frame, contribute to the Cherenkov radiation in the far-field zone. This statement is illustrated in figure 3. The group velocity contour corresponding to the integration contour  $\mathcal{C}_m$  is shown. The color coding is used as in Fig. 2, the same color corresponds to the same frequency and consequently to the same wave vector. Main contributions to the integral (26) for two different observation directions are depicted. For the direction  $\theta_1$  only one Bloch mode with group velocity  $\mathbf{v}_g^{\nu_1}$  satisfies the stationary phase condition, while for the direction  $\theta_{2/3}$  there are two modes with group velocities  $\mathbf{v}_g^{\nu_2}$  and  $\mathbf{v}_g^{\nu_3}$  fulfilling the condition. There does not exist Bloch modes satisfying the stationary phase condition for forward observation directions characterized by angles smaller than  $\theta_1$ .

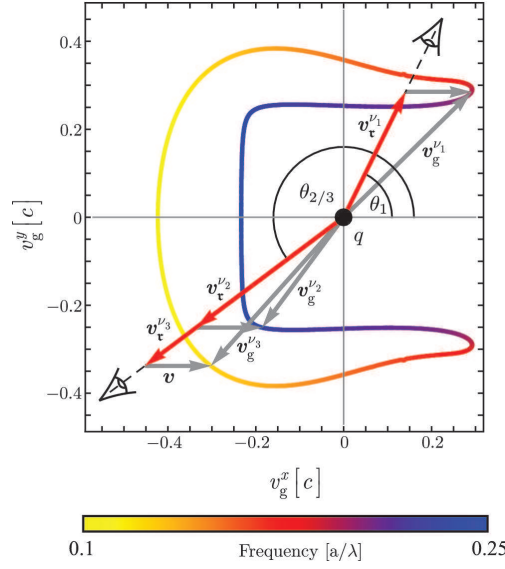


**Figure 3.** Group velocity contour corresponding to the integration contour  $\mathcal{C}_m$ . The main contribution to the Cherenkov radiation in the direction  $\theta_1$  ( $\theta_{2/3}$ ) comes from the Bloch mode(s) with group velocity (velocities)  $\mathbf{v}_g^{\nu_1}$  ( $\mathbf{v}_g^{\nu_2}$  and  $\mathbf{v}_g^{\nu_3}$ ). The same color coding as in Fig. 2 is used.

The integral (26) can be further approximated by expanding the phase  $h(s)$  near the stationary points  $\mathbf{k}(s^\nu) = \mathbf{k}^\nu$  in a Taylor series up to quadratic order

$$h(s) \approx \mathbf{k}^\nu \cdot \mathbf{r} - \omega_n(\mathbf{k}^\nu)t + \frac{1}{2} (\mathbf{r} - \mathbf{v}t) \cdot \frac{\partial^2 \mathbf{k}^\nu}{\partial s^2} (s - s^\nu)^2 \quad (29)$$

and extending the integration range to the whole real axis

$$I_- \approx 2\pi \sum_\nu \frac{\mathbf{e}_n(\mathbf{k}^\nu, \mathbf{r}) c_{nm}(\mathbf{k}^\nu)}{|\mathbf{v}_g(\mathbf{k}^\nu) - \mathbf{v}|} \exp\{i[\mathbf{k}^\nu \cdot \mathbf{r} - \omega_n(\mathbf{k}^\nu)t]\} \cdot \int_{-\infty}^{\infty} ds \exp\left\{\frac{i}{2} \left[ (\mathbf{r} - \mathbf{v}t) \cdot \frac{\partial^2 \mathbf{k}^\nu}{\partial s^2} \right] (s - s^\nu)^2\right\}. \quad (30)$$

Where the summation is taken over all stationary points  $\nu$ . The resulting integral can be evaluated analytically [29]

$$\int_{-\infty}^{\infty} dt e^{ibt^2} = \sqrt{\frac{\pi}{|b|}} \exp\left[i\frac{\pi}{4}\text{sign}(b)\right], \quad (31)$$

which together with the relation

$$(\mathbf{r} - \mathbf{v}t) \cdot \frac{\partial^2 \mathbf{k}^\nu}{\partial s^2} = \text{sign}\left((\mathbf{r} - \mathbf{v}t) \cdot \frac{\partial^2 \mathbf{k}^\nu}{\partial s^2}\right) |(\mathbf{r} - \mathbf{v}t)| \left|\frac{\partial^2 \mathbf{k}^\nu}{\partial s^2}\right| \quad (32)$$

results in the final expression for the Cherenkov electric field in far-field zone for a 2D periodic dielectric medium

$$\mathbf{E}^{(2D)}(\mathbf{r}, t) \approx -\frac{q|\mathbf{v}|}{\epsilon_0 \sqrt{2\pi} |\mathbf{r} - \mathbf{v}t|} \text{Re} \left\{ \sum_{n,\nu} \frac{\mathbf{e}_n(\mathbf{k}^\nu, \mathbf{r}) c_{nm}(\mathbf{k}^\nu)}{|\mathbf{v}_g(\mathbf{k}^\nu) - \mathbf{v}| \sqrt{\mathcal{K}^\nu}} \cdot \exp\{i[\mathbf{k}^\nu \cdot \mathbf{r} - \omega_n(\mathbf{k}^\nu)t]\} \right\}$$



$$\cdot \exp \left\{ i \left[ \frac{\pi}{4} \text{sign} \left( (\mathbf{r} - \mathbf{v}t) \cdot \vec{\mathcal{K}}^\nu \right) \right] \right\}. \quad (33)$$

Here  $\mathcal{K}^\nu = |\vec{\mathcal{K}}^\nu| = \left| \frac{\partial^2 \mathbf{k}^\nu}{\partial s^2} \right|$  is the curvature of the contour  $\mathcal{C}_m$  at the stationary point  $\mathbf{k}^\nu$ . Relation (32) holds because of  $\frac{\partial \mathbf{k}}{\partial s} \perp \frac{\partial^2 \mathbf{k}}{\partial s^2}$  and (27).

### 3.2. 3D periodic media

By introducing a 2D coordinate system with unit vectors  $\frac{\partial \mathbf{k}}{\partial s_1}$  and  $\frac{\partial \mathbf{k}}{\partial s_2}$  tangential to the integration surface  $\mathcal{C}_m$ , the surface integral (23) with  $d = 2$  can be expressed as

$$\begin{aligned} I_- \approx 2\pi \sum_m \int \int ds_1 ds_2 \left| \frac{\partial \mathbf{k}}{\partial s_1} \times \frac{\partial \mathbf{k}}{\partial s_2} \right| \frac{\mathbf{e}_n(\mathbf{k}(\mathbf{s}), \mathbf{r}) c_{nm}(\mathbf{k}(\mathbf{s}))}{|\mathbf{v}_g(\mathbf{k}(\mathbf{s})) - \mathbf{v}|} \\ \cdot \exp [i(\mathbf{k}(\mathbf{s}) \cdot \mathbf{r} - \omega_n(\mathbf{k}(\mathbf{s}))t)]. \end{aligned} \quad (34)$$

where  $\mathbf{s} \in \mathbb{R}^2$ . Similar to the 2D case, the main contribution to the integral comes from the neighborhood of  $k$ -points  $\mathbf{k}(\mathbf{s}^\nu) = \mathbf{k}^\nu$  where the phase  $h(\mathbf{s}) = \mathbf{k}(\mathbf{s}) \cdot \mathbf{r} - \omega_n(\mathbf{k}(\mathbf{s}))t$  is stationary

$$(\mathbf{r} - \mathbf{v}t) \cdot \frac{\partial \mathbf{k}^\nu}{\partial s_i} = 0, \quad (35)$$

with  $i \in \{1, 2\}$ . Choosing a local coordinate system at the stationary point  $\mathbf{k}^\nu$  with basis vectors  $\frac{\partial \mathbf{k}}{\partial \xi_1}$  and  $\frac{\partial \mathbf{k}}{\partial \xi_2}$  along the main directions of the surface curvatures the following form of the Taylor expansion of the phase  $h(\mathbf{s})$  can be used to evaluate the integral (34)

$$\begin{aligned} h(\xi_1, \xi_2) \approx \mathbf{k}^\nu \cdot \mathbf{r} - \omega_n(\mathbf{k}^\nu)t \\ + \frac{1}{2} (\mathbf{r} - \mathbf{v}t) \cdot \left( \frac{\partial^2 \mathbf{k}^\nu}{\partial \xi_1^2} (\xi_1 - s_1^\nu)^2 + \frac{\partial^2 \mathbf{k}^\nu}{\partial \xi_2^2} (\xi_2 - s_2^\nu)^2 \right), \end{aligned} \quad (36)$$

where  $\frac{\partial^2 \mathbf{k}^\nu}{\partial \xi_1^2}$  and  $\frac{\partial^2 \mathbf{k}^\nu}{\partial \xi_2^2}$  are the main curvatures  $\mathcal{K}_1^\nu$  and  $\mathcal{K}_2^\nu$  of the integration surface  $\mathcal{C}_m$ . The integration limit is then extended to the whole real plane. Using twice the relation (31) the Cherenkov electric field in far-field zone for a 3D periodic dielectric medium reads

$$\begin{aligned} \mathbf{E}^{(3D)}(\mathbf{r}, t) \approx - \frac{q|\mathbf{v}|}{2\pi\epsilon_0|\mathbf{r} - \mathbf{v}t|} \text{Re} \left\{ \sum_{n,\nu} \frac{\mathbf{e}_n(\mathbf{k}^\nu, \mathbf{r}) c_{nm}(\mathbf{k}^\nu)}{|\mathbf{v}_g(\mathbf{k}^\nu) - \mathbf{v}| \sqrt{\mathcal{K}_1^\nu \mathcal{K}_2^\nu}} \right. \\ \cdot \exp \{ i[\mathbf{k}^\nu \cdot \mathbf{r} - \omega_n(\mathbf{k}^\nu)t] \} \\ \cdot \exp \left\{ i \left[ \frac{\pi}{4} \text{sign} \left( (\mathbf{r} - \mathbf{v}t) \cdot \vec{\mathcal{K}}_1^\nu \right) \right] \right\} \\ \left. \cdot \exp \left\{ i \left[ \frac{\pi}{4} \text{sign} \left( (\mathbf{r} - \mathbf{v}t) \cdot \vec{\mathcal{K}}_2^\nu \right) \right] \right\} \right\}, \end{aligned} \quad (37)$$

with the product of the main curvatures  $\mathcal{K}_1^\nu \mathcal{K}_2^\nu$  being the Gaussian curvature of the surface  $\mathcal{C}_m$  defined by the generalized Cherenkov condition (25). The vectors  $\vec{\mathcal{K}}_i$  are defined by  $\vec{\mathcal{K}}_i = \frac{\partial^2 \mathbf{k}^\nu}{\partial \xi_i^2}$ .

#### 4. Discussion and numerical examples

Formulas (24), (33) and (37) constitute the main result of the present work. In the far-field zone the electric field generated by a point (line) charge uniformly moving in a 3D (2D) periodic medium is dominated by a small number of Bloch eigenmodes of the medium. To calculate the far-field, these Bloch modes (their wave vectors) should be calculated as a solution of the generalized Cherenkov condition (25). In turn, the spatial variation of the Cherenkov radiation is dominated (i) by the interference of these Bloch modes at the observation point and (ii) by the topology of the dispersion relation at the Cherenkov surface (contour) in Eqs. (24) and (37) (Eqs. (24) and (33)).

In what follows, we apply formulas (24) and (33) to study the spatial distribution of Cherenkov radiation in the 2D photonic crystal depicted in Fig. 1. The line charge oriented perpendicular to the periodicity plane of the crystal moves along the  $x$ -axis with a velocity  $v = 0.15c$ , staying always in the space between air holes. The corresponding current density (6) couples only to Bloch eigenmodes with an electric field polarized in the periodicity plane (TE polarization). The first TE photonic band of the considered crystal is presented in figure 2. The band structure as well as group velocities and Bloch eigenmodes were calculated using the plane wave expansion method [30].

In order to calculate both the electric field (24) and its approximation (33) the set of wave vectors contributing to the far-field should be calculated. This set can be found as a numerical solution of the generalized Cherenkov condition (dashed line in Fig. 2). In contrast to the homogeneous medium case, such a solution does exist for an arbitrary charge velocity [27].

Having the set of wave vectors  $\mathcal{C}_m$ , the Bloch modes  $\mathbf{e}_{\mathbf{k}n}$  and the Fourier coefficient  $c_{nm}(\mathbf{k})$  can be calculated. The Fourier coefficients  $c_{nm}(\mathbf{k})$  give the coupling strength between the current associated with the moving charge and the Bloch eigenmodes. As it can be seen from the definition (14), with increasing index  $|m|$  the Fourier coefficients become smaller, reducing the contribution of the higher frequencies to the Cherenkov radiation in the far-field zone. Finally, the Cherenkov field (24) can be calculated by direct numerical integration.

To calculate the stationary phase approximation of the far-field (33), stationary wave vectors  $\mathbf{k}^\nu$  should be calculated for a given observation direction  $\mathbf{r} - \mathbf{v}t$ . This can be done by parameterizing the Cherenkov contour by the arc length  $s$  and looking for all Bloch modes whose group velocities (Fig. 3) satisfy the stationary phase condition  $(\mathbf{v}_g(\mathbf{k}^\nu) - \mathbf{v}) \uparrow\uparrow (\mathbf{r} - \mathbf{v}t)$ . Furthermore, the Bloch modes, the Fourier coefficient and the curvature of the Cherenkov contour (see Appendix) should be calculated and summed for these stationary points only. This reduce the computational demands considerably.

In figure 4, a numerical calculations of the stationary phase approximation of the far-field is presented for  $v = 0.15c$ . The  $E_x(\mathbf{r}, t = 0)$  and  $E_y(\mathbf{r}, t = 0)$  components of the electric field are shown in the upper halves of the top and bottom panels, respectively. Only contributions from the first three sections of the Cherenkov contour corresponding to  $m = 0, -1, -2$  have been analyzed. In the case of a homogeneous medium, the standard Cherenkov condition would impose a minimal charge velocity above which Cherenkov radiation is possible  $v_{\min} \geq c/n_{\text{eff}} \approx 0.457c$ . Here an effective refractive index of the considered periodic medium is asymptotically equal to  $n_{\text{eff}} = \sqrt{\varepsilon_{\text{eff}}} \approx 2.186$ . Although the velocity of the line charge is considerably smaller

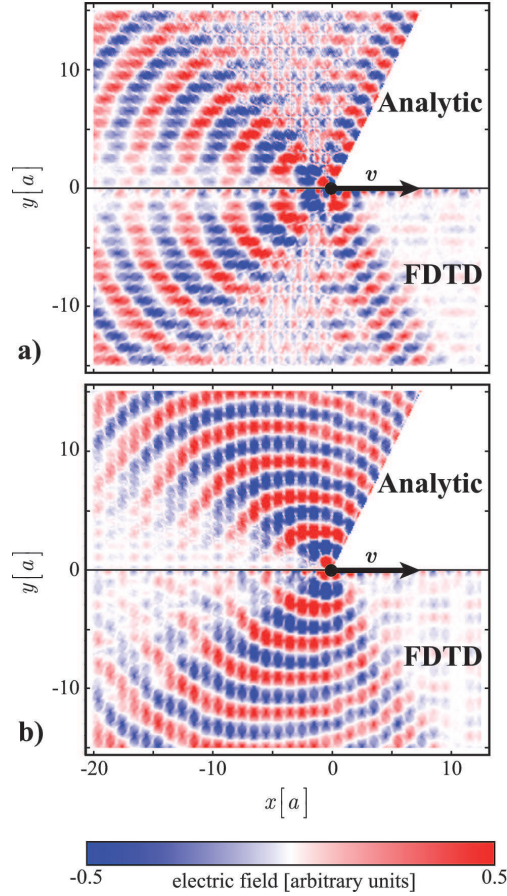


**Figure 4.**  $E_x(\mathbf{r}, t = 0)$  (top panel) and  $E_y(\mathbf{r}, t = 0)$  (bottom panel) components of the Cherenkov electric field for a charge velocity  $v = 0.15c$ . The results of the stationary phase approximation (33) and direct numerical integration using FDTD methods are shown.

than  $v_{\min}$ , in the periodic medium the non-evanescent field can be clearly seen far apart from the charge trajectory (Fig. 4). Another characteristic feature of the spatial distribution of the Cherenkov radiation for  $v = 0.15c$  is a backward-pointing radiation cone [26]. The field in the forward direction for observation angles smaller than  $\theta_1$  is zero.

The zero field within the backward-pointing radiation cone is associated with the absence of stationary solutions for observation directions in the cone (Fig. 3). This is a direct consequence of the stationary phase approximation. In figure 5 a), the stationary phase approximation of the far-field 10 lattice constants apart from the trajectory is compared with the direct numerical integration of the integral representation of the field (24). An excellent agreement between these two solutions can be seen up to the Cherenkov cone  $\theta_1$ , where the stationary phase approximation breaks down. The cone angle corresponds to the fold in the group velocity contour (Fig. 3). The curvature of the Cherenkov contour is zero at the corresponding wave vector and the Taylor expansion (29) fails to reproduce the contour accurately in the

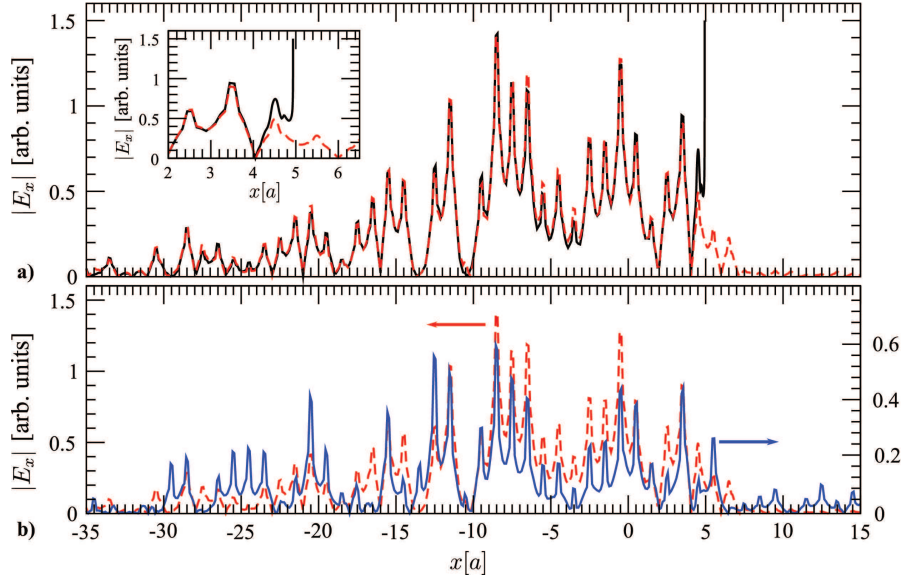


**Figure 5.** Comparison of the integral representation of the far-field (24) (dashed red line) with the stationary phase approximation (33) (black solid line) and FDTD calculations (blue solid line). An absolute value of the horizontal component of the electric field is shown 10 lattice constants apart from the charge trajectory.

vicinity of this point. Zero curvature leads to the diverging field (Fig. 5-inset). The field calculated with Eq. (24) is small but finite in forward directions.

To substantiate our analytical calculations, a direct numerical integration of Maxwell's equations (1-2) using rigorous finite-differences time-domain (FDTD) method [31] has been performed. The corresponding FDTD field distributions are presented in the lower halves of the top and bottom panels of figure 4.  $200a \times 70a$  lattice of holes with discretization  $\Delta = a/18$  has been used for the FDTD calculation. The simulation domain is surrounded by a  $3a$ -wide perfectly matched layer (PML). The integration time step is set to 98% of the Courant value. In order to describe a continuous movement of the charge, the source (6) is modeled by a discrete Gaussian in the  $x$ -direction with a standard deviation  $\sigma = \Delta$  and by an appropriately normalized Kronecker delta in the  $y$ -direction

$$j(x_i\Delta, y_j\Delta) = \frac{\delta_{jk}}{\sqrt{2\pi}\Delta^2} \exp\left[-\frac{(x_i\Delta - vt)^2}{2\Delta^2}\right]$$

where  $y_k = 35a$  is the center of the crystal in the vertical direction. In order to compare directly FDTD results with the predictions of formulas (24) and (33), the static contribution as well as the higher frequency contributions to the FDTD field have been filtered out. An overall good agreement between the results of the analytical and direct numerical calculation is obtained (Fig. 4 and 5). The FDTD calculation follows nicely the main characteristic of the analytically predicted field. The difference in the absolute values between FDTD and analytical calculations (Fig. 5) can be associated with the residual reflections from the perfectly matched layer.

## 5. Conclusion

In conclusion, we have developed an analytical theory of the Cherenkov radiation in the far-field zone. The field far apart from the charge trajectory can be calculated as a surface (contour) integral over a small fraction of the first Brillouin Zone in a 3D (2D) dielectric medium. We have shown that the main contribution to this integral comes from a small and discrete number of  $k$ -points. This opens the possibility to calculate the integral approximately, but with high accuracy. We have also shown, that the spatial variation of the Cherenkov radiation in the far-field is due to the interference of a few Bloch eigenmodes as well as the topological properties of the Cherenkov surface (contour). This has been defined as a manifold of all  $k$ -points contributing to the Cherenkov radiation for a given charge velocity. Simple formulas have been derived for the Cherenkov far-field both in 3D and 2D cases. We have compared the developed analytical theory with numerically rigorous FDTD calculations. A good agreement between these two methods has been demonstrated.

## Acknowledgments

We are grateful to Sergei Zhukovsky and Fuh Chuo Evaristus for fruitful discussions. Financial support from the Deutsche Forschungsgemeinschaft (DFG FOR 557) is acknowledged.

## Appendix

To calculate the curvature using its definition

$$\mathcal{K}(s) = \left| \frac{\partial^2 \mathbf{k}(s)}{\partial s^2} \right|$$

one should numerically evaluate the second derivative of the wave vector  $\mathbf{k}(s)$  on the Cherenkov contour. This is typically associated with a large numerical error. In what follows we propose to use an alternative method to calculate the curvature which usually results in smaller numerical error and involves calculations of the first derivative of the wave vector on the contour and the second derivatives of the dispersion relation  $\omega_n(\mathbf{k})$ .

Taking the derivative of (28) with respect to  $s$  we obtain

$$\frac{\partial^2 \mathbf{k}}{\partial s^2} \cdot (\mathbf{v}_g(\mathbf{k}(s)) - \mathbf{v}) + \frac{\partial \mathbf{k}}{\partial s} \cdot \frac{\partial}{\partial s} \mathbf{v}_g(\mathbf{k}(s)) = 0 \quad (\text{A.1})$$

The second term in (A.1) can be rewritten as

$$\begin{aligned} \frac{\partial \mathbf{k}}{\partial s} \cdot \frac{\partial}{\partial s} \mathbf{v}_g(\mathbf{k}(s)) &= \sum_i \frac{\partial k_i}{\partial s} \left[ \frac{\partial}{\partial s} \frac{\partial}{\partial k_i} \omega_n(\mathbf{k}) \right] \\ &= \sum_{i,j} \frac{\partial k_i}{\partial s} \frac{\partial^2}{\partial k_j \partial k_i} \omega_n(\mathbf{k}) \frac{\partial k_j}{\partial s} \\ &= \left( \frac{\partial \mathbf{k}}{\partial s} \right)^T \mathcal{H}_{\omega_n}(\mathbf{k}) \frac{\partial \mathbf{k}}{\partial s} = \mathcal{M}, \end{aligned}$$

where  $\mathcal{H}_{\omega_n}(\mathbf{k})$  is a Hessian matrix of the dispersion relation  $\omega_n(\mathbf{k})$ . We can now rewrite (A.1) in the form

$$\frac{\partial^2 \mathbf{k}}{\partial s^2} \cdot (\mathbf{v}_g(\mathbf{k}(s)) - \mathbf{v}) = \mathcal{M}$$

or

$$\mathcal{K} |\mathbf{v}_g(\mathbf{k}(s)) - \mathbf{v}| \text{sign} \left[ \vec{\mathcal{K}} \cdot (\mathbf{v}_g(\mathbf{k}(s)) - \mathbf{v}) \right] = \mathcal{M}$$

with  $\vec{\mathcal{K}} = \frac{\partial^2 \mathbf{k}}{\partial s^2}$ . Finally the following expression for the curvature is obtained

$$\mathcal{K} = \frac{|\mathcal{M}|}{|\mathbf{v}_g(\mathbf{k}(s)) - \mathbf{v}|}. \quad (\text{A.2})$$

- [1] Joannopoulos J D, Meade R D and Winn J N 1995 *Photonic Crystals: Molding the Flow of Light* (Princeton:Princeton University Press)
- [2] Sakoda K 2001 *Optical Properties of Photonic Crystals* (Berlin: Springer)
- [3] Bykov V P 1972 *Sov. Phys. JETP* **35** 269
- [4] Yablonoitch E 1987 *Phys. Rev. Lett.* **58** 2059
- [5] John S and Wang J 1990 *Phys. Rev. Lett.* **64** 2418
- [6] Russell P St J 1986 *Appl. Phys. B: Photophys. Laser Chem.* **39** 231
- [7] Zengerle J 1987 *J. Mod. Opt.* **34** 1589
- [8] Kosaka H, Kawashima T, Tomita A, Notomi M, Tamamura T, Sato T and Kawakami S 1998 *Phys. Rev. B* **58** R10096
- [9] Kosaka H, Kawashima T, Tomita A, Notomi M, Tamamura T, Sato T and Kawakami S 1999 *Appl. Phys. Lett.* **74**
- [10] Etchegoin P and Phillips R T 1996 *Phys. Rev. B* **53** 12674
- [11] Chigrin D N and Sotomayor Torres C M 2001 *Opt. Spectrosc.* **91** 484
- [12] Chigrin D N 2004 *Phys. Rev. E* **70** 056611
- [13] Cherenkov P A 1934 *Dokl. Acad. Nauk SSSR* **2** 457
- [14] Jelley J V 1958 *Cherenkov Radiation and its Applications* (New York:Pergamon)
- [15] Fermi E 1940 *Phys. Rev.* **57** 485
- [16] Afanasiev G N, Kartavenko V G and Magar E N 1999 *Physica* **B269** 95
- [17] Carusotto I, Artoni M, La Rocca G C and Bassani F 2001 *Phys. Rev. Lett.* **87** 064801
- [18] Artoni M, Carusotto I, La Rocca G C and Bassani F 2003 *Phys. Rev. E* **67** 046609
- [19] Garcia de Abajo F J and Blanco L A 2003 *Phys. Rev. B* **67** 125108
- [20] Ochiai T and Ohtaka K 2004 *Phys. Rev. B* **69** 125106
- [21] Ochiai T and Ohtaka K 2004 *Phys. Rev. B* **69** 125107
- [22] Yamamoto et al. 2004 *Phys. Rev. E* **69** 045601(R)
- [23] Ochiai T and Ohtaka K 2006 *Opt. Express* **14** 7378
- [24] Garcia de Abajo F J, Pattantyus-Abraham A G, Zabala N, Rivacoba A, Wolf M O and Echenique P M 2003 *Phys. Rev. Lett.* **91** 143902
- [25] Garcia de Abajo F J, Rivacoba A, Zabala N and Echenique P M 2003 *Phys. Rev. B* **68** 205105
- [26] Luo C, Ibanescu M, Johnson S G and Joannopoulos J D 2003 *Science* **299** 368
- [27] Kremers C, Chigrin D N and Kroha J 2009 *Phys. Rev. A* **79** 013829
- [28] Dowling J P and Bowden C M 1992 *Phys. Rev. A* **46** 612
- [29] Jeffrey A and Zwillinger D 2007 *Table of Integrals, Series and Products* (Academic Press)
- [30] Johnson S G and Joannopoulos J D 2001 *Opt. Express* **8** 173-190
- [31] Taflove A 1995 *Computational Electrodynamics: The Finite-Difference Time-Domain Method* (Norwood: Artech House)